Study on the Structural Properties and CO_2 Reduction Mechanism of Cu_{13} Nanoparticles Supported on Carbon Nanotubes and Defective Graphene

Xin-Long Zhang, Xiao-Min Liang, Dong-Hui Xu, Wen-Jun Jiang, Lai-Cai Li*,

College of Chemistry and Material Science, Sichuan Normal University, Chengdu 610068, China

E-mail: lilcmail@163.com

Content

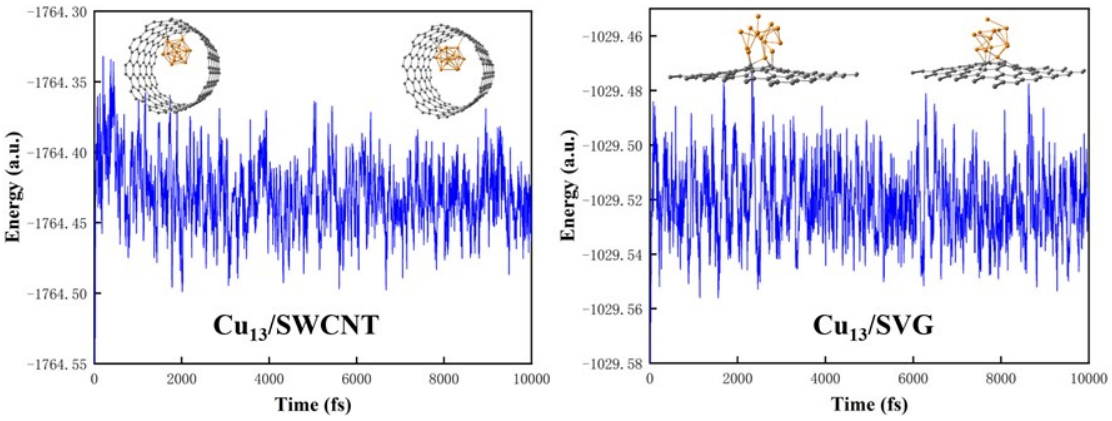

Fig.S1. The AIMD simulations of Cu_{13}/SWCNT and Cu_{13}/SVG at 298.15 K for a duration of 10 ps.

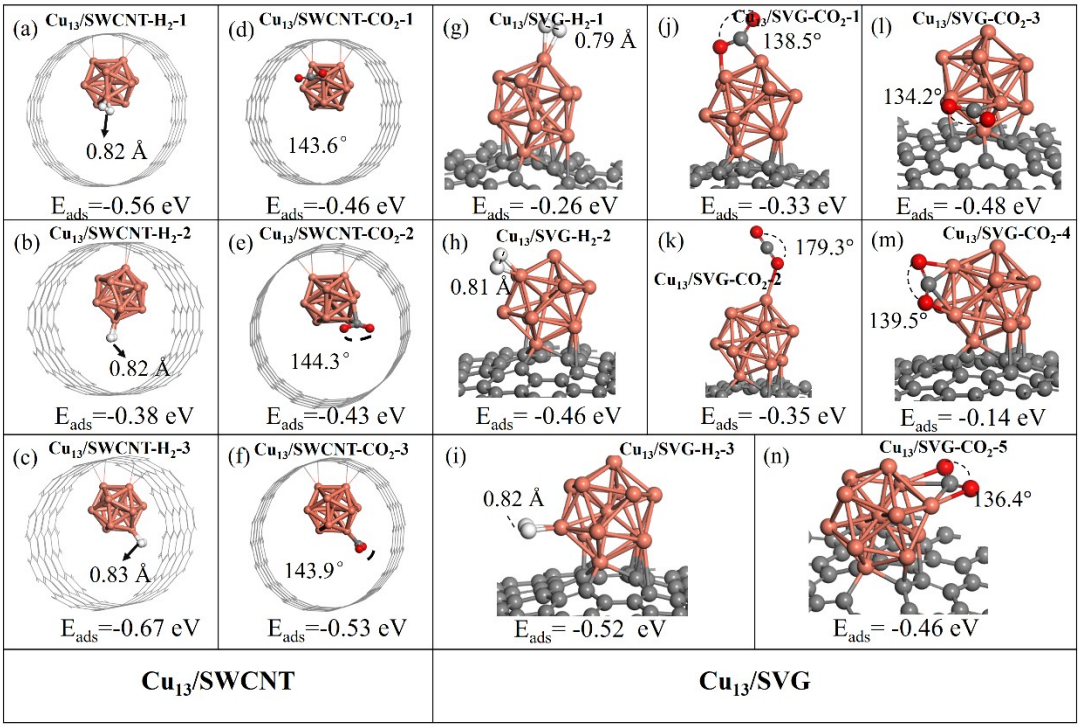

Fig.S2. The adsorption configurations of CO_2 and H_2 on Cu_{13}/SWCNT(a~f) and Cu_{13}/SVG(g~n).

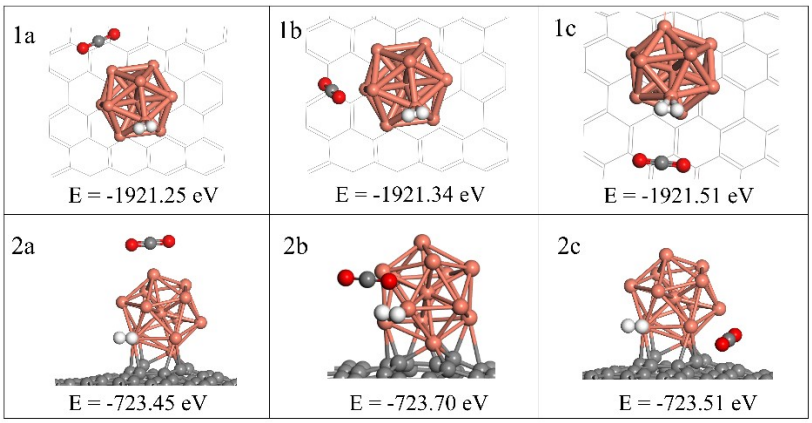

Fig.S3. CO_2 and H_2 co-adsorption sites on Cu_{13}/SWCNT(1a~1c) and Cu_{13}/SVG(2a~2c).

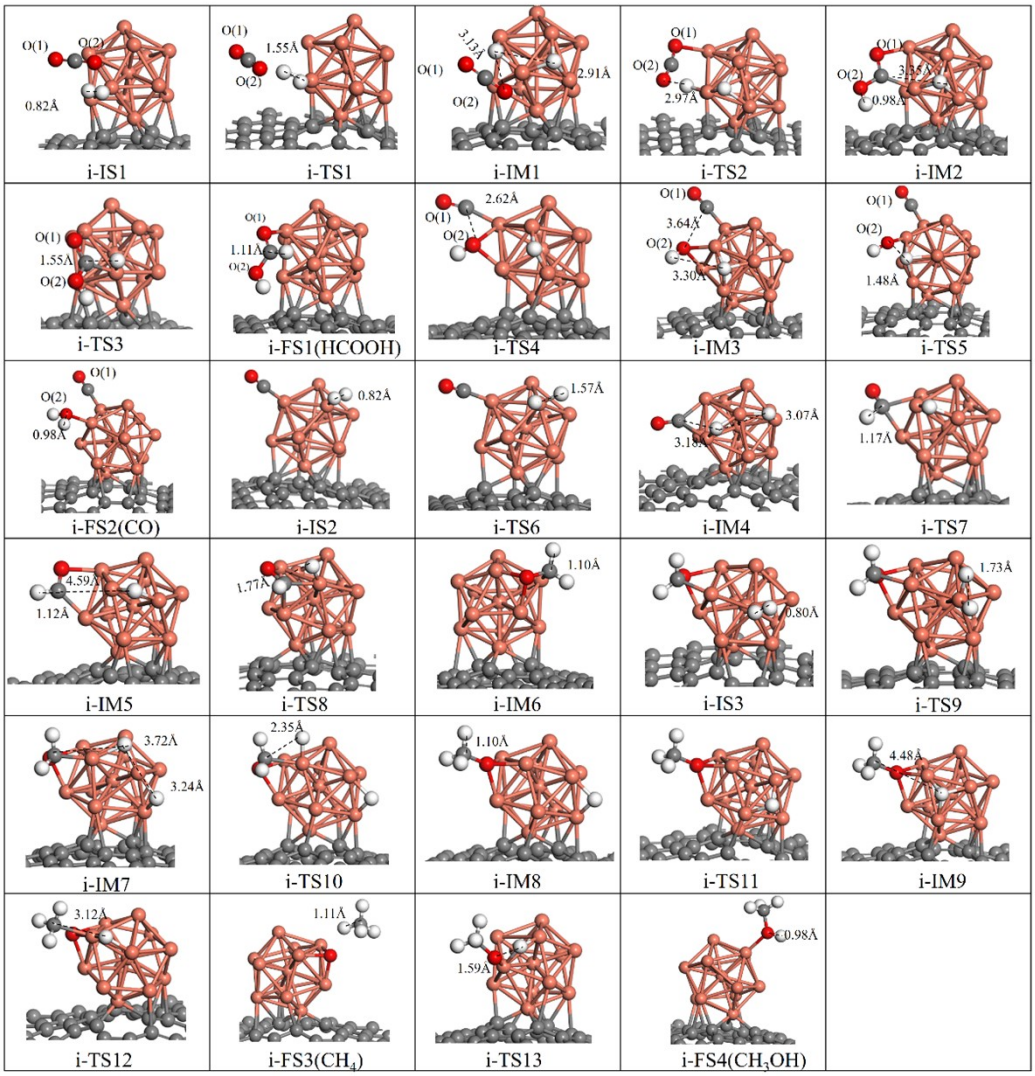

Fig.S4. Optimized configurations of key intermediates for CO_2 reduction via the RWGS+CO hydrogenation pathway on the Cu_{13}/SVG catalyst

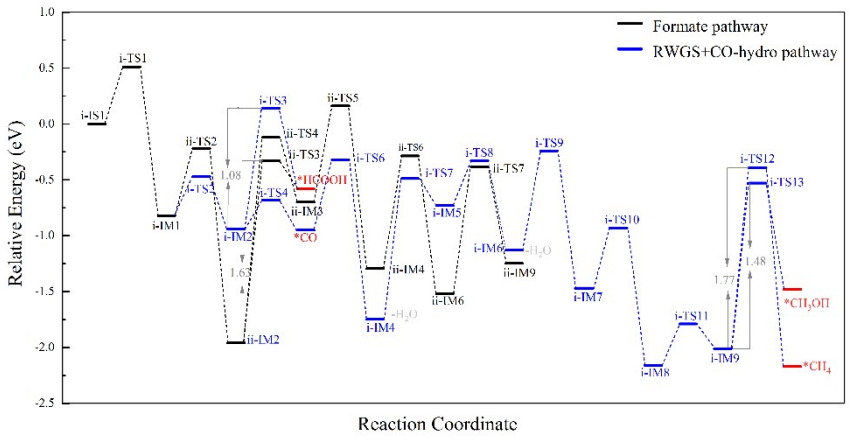

Fig.S5. Energy profiles for CO_2 reduction over Cu_{13}/SVG via the RWGS+CO hydrogenation and formate pathways

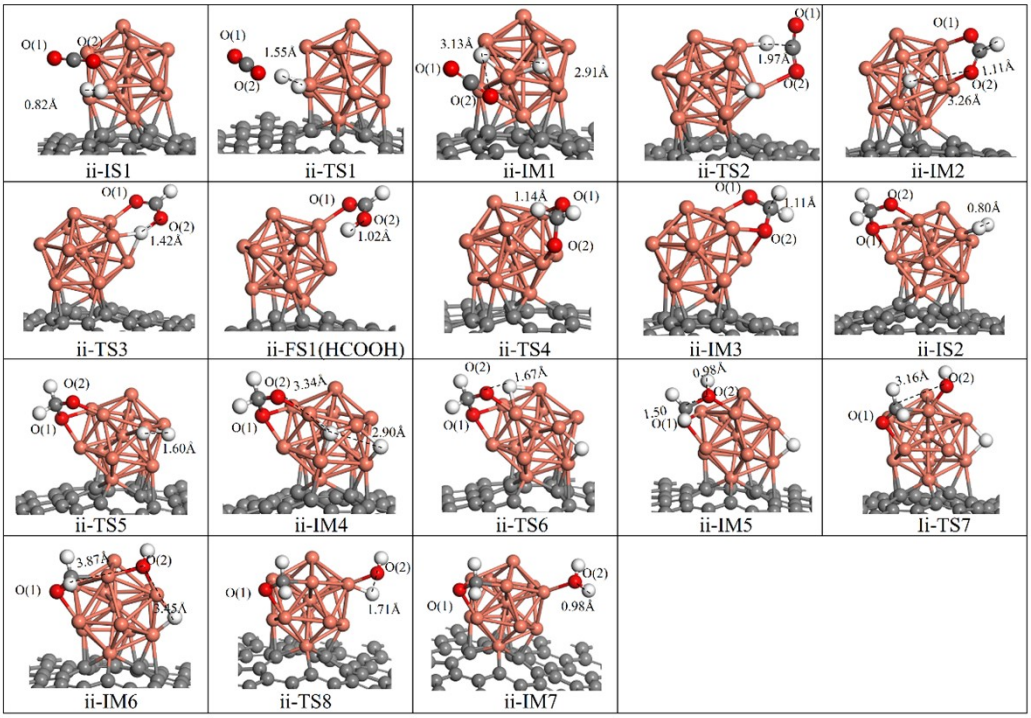

Fig.S6. Optimized structures of each reaction state for CO_2 reduction via the FBF pathway catalyzed by Cu_{13}/SVG.

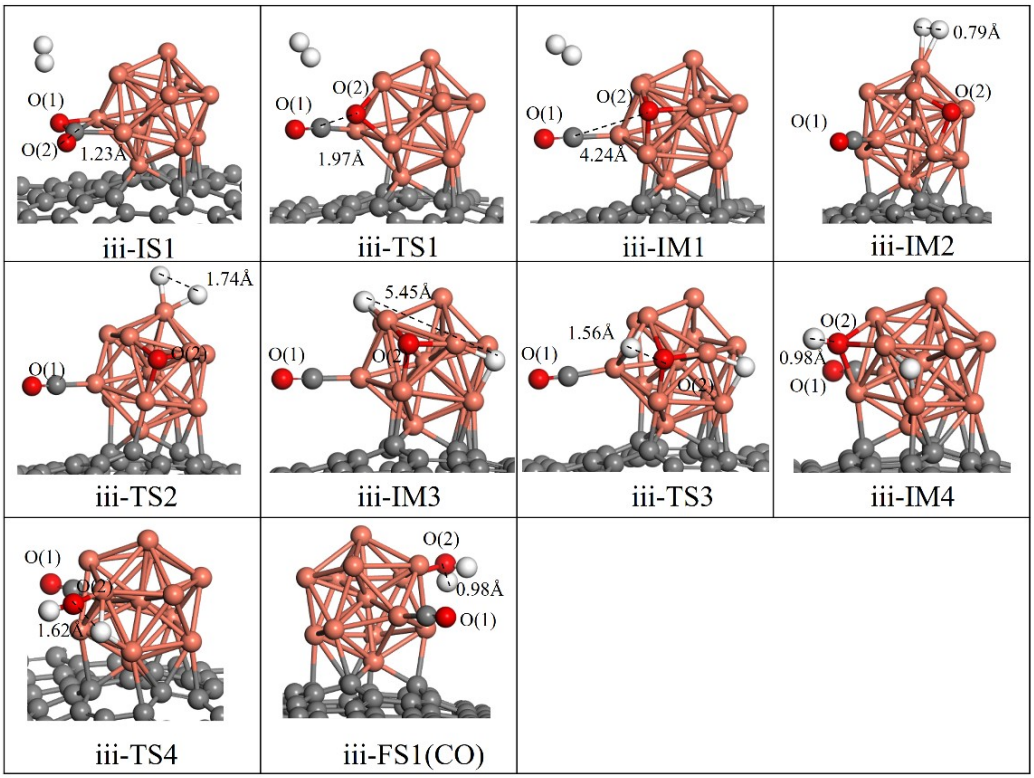

Fig.S7. Various adsorption site configurations of Cu_{13}/SVG catalyzing CO_2 reduction along the FBB pathway.

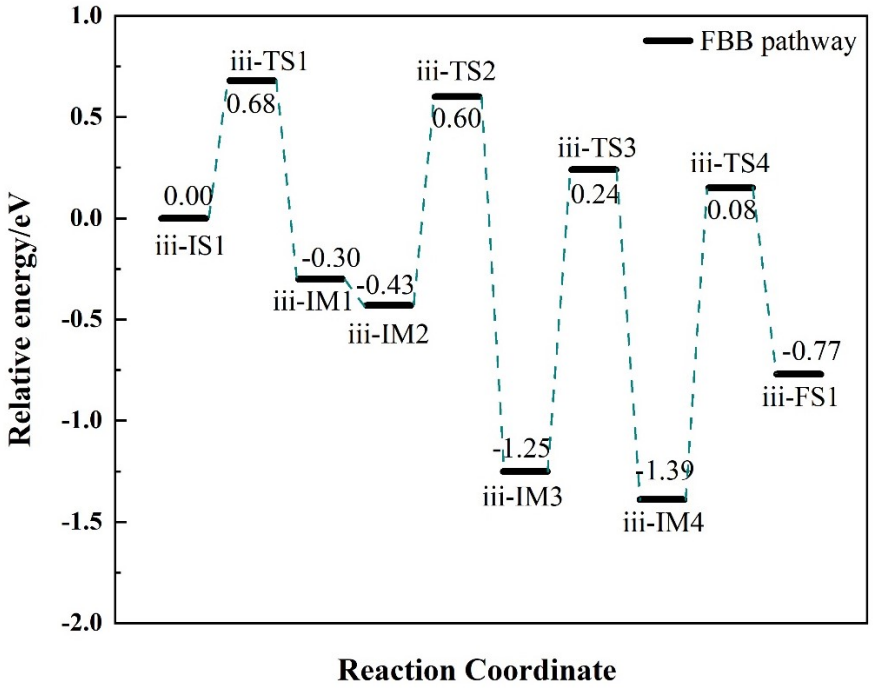

Fig.S8. Energy level diagram for the CO_2 reduction to *CO catalyzed by Cu_{13}/SVG along the FBB pathway.

Table S1. Energy barriers (E_b), reaction enthalpies (ΔH), and vibrational frequencies (v) for each adsorption site during CO_2 reduction via the RWGS+CO hydrogenation pathway on Cu_{13}/SVG.

Elementary process	Material	ΔH (eV)	E_b (eV)	v (i cm^{-1})
	i-IS1			
$*H_2 \rightarrow 2*H$	i-TS1	-0.82	0.51	840.77
	i-IM1			
$*CO_2 \rightarrow *COOH$	i-TS2	-0.12	0.35	150.67
	i-IM2			
$*COOH \rightarrow HCOOH$	i-TS3	0.66	1.08	63.02
	i-FS1			
$*COOH \rightarrow *CO$	i-TS4	-0.49	0.26	281.74
	i-IM3			
$*OH+*H \rightarrow H_2O$	i-TS5	0.47	1.43	1902.87
	i-FS2			
	i-IS2			
$H_2 \rightarrow *2H$	i-TS6	-0.80	0.63	865.81
	i-IM4			
$*CO \rightarrow *CHO$	i-TS7	1.02	1.26	330.79
	i-IM5			
$*CHO \rightarrow *CH_2O$	i-TS8	-0.41	0.40	694.40
	i-IM6			
	i-IS3			
$H_2 \rightarrow *2H$	i-TS9	-0.34	0.89	756.57
	i-IM7			
$*CH_2O \rightarrow *CH_3O$	i-TS10	-0.68	0.54	257.50
	i-IM8			
*H transfer	i-TS11	0.15	0.36	244.87
	i-IM9			
$*CH_3O \rightarrow CH_3OH$	i-TS13	-0.16	1.77	526.00
	i-FS4			
$*CH_3O \rightarrow CH_4$	i-TS12	0.53	1.48	562.68
	i-FS3			

Table S2. Energy barriers (E_b), reaction enthalpies (ΔH), and vibrational frequencies (v) for each intermediate state during CO_2 reduction via the FBF pathway over the Cu_{13}/SVG catalyst.

Elementary process	Material	ΔH(eV)	E_b (eV)	v(i cm^{-1})
	ii-IS1			
H_2→2*H	ii-TS1	-0.82	0.51	840.77
	ii-IM1			
CO_2→*HCOO	ii-TS2	-1.14	0.60	393.79
	ii-IM2			
*HCOO→HCOOH	ii-TS3	1.38	1.63	1068.63
	ii-FS1			
HCOO→H_2COO	ii-TS4	1.26	1.84	262.79
	ii-IM3			
	ii-IS2			
H_2→2*H	ii-TS5	-0.60	0.86	853.15
	ii-IM4			
H_2COO→H_2COOH	ii-TS6	-0.22	1.01	679.09
	ii-IM5			
H_2COOH→H_2CO	ii-TS7	0.27	1.13	88.13
	ii-IM6			
*OH→H_2O	ii-TS8	0.34	1.95	992.37
	ii-IM7			

Table S3. Energy barriers (E_b), reaction enthalpies (ΔH), and frequencies (v) of the adsorption sites during CO_2 reduction catalyzed by Cu_{13}/SVG along the FBB pathway.

Elementary process	Material	ΔH(eV)	E_b (eV)	v (i cm^{-1})
	iii-IS1			
CO_2→*CO+O	iii-TS1	-0.30	0.68	233.68
	iii-IM1			
H_2→*H_2	iii-IM2	-0.13		
H_2→2*H	iii-TS2	-0.82	1.03	752.71

	iii-IM3			
*H+*O→*OH	iii-TS3	-0.13	1.49	1242.94
	iii-IM4			
*H+*OH→H_2O	iii-TS4	0.61	1.54	638.26
	iii-FS1			